Robot Cartesian Compliance Variation for Safe Kinesthetic Teaching using Safety Control Barrier Functions

Salt Ducaju, Julian; Olofsson, Björn; Robertsson, Anders; Johansson, Rolf

Published in:
Proc. 2022 IEEE 18th International Conference on Automation Science and Engineering (CASE), August 20-24, 2022. Mexico City, Mexico

DOI:
10.1109/CASE49997.2022.9926525

2022

Document Version:
Peer reviewed version (aka post-print)

Robot Cartesian Compliance Variation for Safe Kinesthetic Teaching using Safety Control Barrier Functions

Julian M. Salt Ducaju, Björn Olofsson, Anders Robertsson, Rolf Johansson

***Abstract*— Kinesthetic teaching allows human operators to reprogram part of a robot's trajectory by manually guiding the robot. To allow kinesthetic teaching, and also to avoid any harm to both the robot and its environment, Cartesian impedance control is here used for trajectory following. In this paper, we present an online method to modify the compliant behavior of a robot toward its environment, so that undesired parts of the robot's workspace are avoided during kinesthetic teaching. The stability of the method is guaranteed by a well-known passivity-based energy-storage formulation that has been modified to include a strict Lyapunov function, *i.e.*, its time derivative is a globally negative-definite function. Safety Control Barrier Functions (SCBFs) that consider the rigid-body dynamics of the robot are formulated as inequality constraints of a quadratic optimization (QP) problem to ensure forward invariance of the robot's states in a safe set. An experimental evaluation using a Franka Emika Panda robot is provided.**

I. Introduction

Physical Human–Robot Interaction (pHRI) has become a popular topic in the robotics community, since it addresses the recent trend in the manufacturing industry to replace mass production for mass customization [1]. As part of this change of paradigm, human operators have become direct collaborators in robotic tasks, and robots that are compliant toward their environment have gained relevance.

An interesting application of human collaboration in robotics is to reprogram part of the robot's trajectory [2] by manually guiding the robot, which is known as kinesthetic teaching [1]. However, the workspace that humans and robots share may not be entirely available, *e.g.*, if another robot arm is occupying part of the workspace, or if there is sensitive equipment in the workspace. Then, the robot's compliant behavior toward its environment should be modified so that the human operator cannot guide the robot to unsafe situations. In addition, the compliance variations must be done in such a way that the stability of the robot's controller is ensured. Passivity-based energy storage has been used previously to provide a stable variation of the impedance parameters of a robot [3], [4].

Moreover, Safety Control Barrier Functions (SCBFs) have gained attention in recent years [5]–[10], because they provide more formal guarantees for obstacle avoidance than the artificial potential-field methods used in the past for this purpose [11]. Safety control barrier functions provide safety by enforcing forward invariance of a set, *i.e.*, SCBFs ensure that a system does not leave a safe set [5]. They can be formulated as inequality constraints of a quadratic optimization (QP) problem to modify the input to the system [5], [6]. Additionally, SCBFs have been used to perform a minimally-invasive modification of the robot's behavior to avoid safety threats, such as obstacle collisions [7]–[10].

In this paper, we address the problem of safe kinesthetic teaching by modifying the Cartesian compliant behavior of a robot with respect to its environment in a strictly stable manner, such that we can ensure that the robot's end-effector avoids undesired parts of its workspace. Safety control barrier functions that consider the rigid-body dynamics of the robot are used as inequality constraints of a quadratic optimization problem to online modify the robot's compliance behavior in a minimally-invasive way, so that the human operator can still manipulate the robot while avoiding any safety threat.

The paper is organized as follows: Sec. II introduces relevant mathematical concepts that are used in our method. Then, Sec. III presents the method for solving the described problem. Section IV explains the experiments performed, and Sec. V presents the results obtained. Finally, a discussion is included in Sec. VI and conclusions are drawn in Sec. VII.

II. Mathematical Background

In this section, we discuss two relevant mathematical concepts. First, SCBFs for safe set forward invariance. Second, passivity-based energy storage for stable variation of the robot compliant behavior with respect to its environment.

A. Safety Control Barrier Functions (SCBFs)

Consider a nonlinear control-affine system:

$$\dot{x} = f(x) + g(x)u \tag{1}$$

that has closed-loop system dynamics with a state-feedback controller k according to

$$\dot{x} = f_{cl}(x,t) = f(x) + g(x)k(x,t) \tag{2}$$

Moreover, define a safe set $\mathcal{C}$, with boundary $\partial\mathcal{C}$ and interior $\text{Int}(\mathcal{C})$, as [5]

$$\mathcal{C} = \{x \in \mathbb{R}^n \mid h(x) \geq 0\} \tag{3}$$

$$\partial\mathcal{C} = \{x \in \mathbb{R}^n \mid h(x) = 0\} \tag{4}$$

$$\text{Int}(\mathcal{C}) = \{x \in \mathbb{R}^n \mid h(x) > 0\} \tag{5}$$

For $\mathcal{C}$ to be forward invariant [5],

$$\sup_{u \in \mathcal{U}} [L_f h(x) + L_g h(x) u] \geq -\kappa(h(x)) \tag{6}$$

The authors are members of the ELLIIT Strategic Research Area at Lund University. This work was partially supported by the Wallenberg AI, Autonomous Systems and Software Program (WASP).

J. M. Salt Ducaju, julian.salt_ducaju@control.lth.se, B. Olofsson, A. Robertsson, and R. Johansson are with the Department of Automatic Control, LTH, Lund University, Lund, Sweden.

for all $x \in \mathcal{D}$, being h the SCBF, $h : \mathcal{D} \to \mathbb{R}$ with $\mathcal{C} \subseteq \mathcal{D} \subset \mathbb{R}^n$, κ an extended class-$\mathcal{K}_\infty$ function (strictly monotonically increasing), $L_f h(x) = (\partial h/\partial x) f(x)$, and $L_g h(x) = (\partial h/\partial x) g(x)$. Also, the authors in [6] highlight the possibility of choosing $\kappa(h) = \gamma h^Z$ ($\gamma > 0$) for any positive odd integer Z.

Furthermore, a quadratic optimization (QP) problem can be formulated to minimize the difference between the input to the system, u, and the nominal state-feedback controller in (2), k^d, while using SCBFs to formulate an inequality constraint that allows obstacle avoidance [5]:

$$\begin{aligned} k(x,t) = \arg\min_{u \in \mathbb{R}^m} & \frac{1}{2} \left|\left| u - k^d(x,t) \right|\right|_2^2 \\ \text{s.t.} \;\; & \dot{h}(x,t,u) \geq -\kappa(h(x,t)) \end{aligned} \tag{7}$$

B. Passivity-Based Energy Storage

Energy storage has previously been used to handle stiffness variations in robots [3], [4]. This formulation is based on the idea of keeping the energy introduced to the system lower that the energy dissipated by the system. The energy dissipated by the system's damping is stored in an energy reservoir with state $z(t) \in \mathbb{R}$ and dynamics

$$\dot{z} = \frac{\varphi}{z} P_D - \frac{\sigma}{z} P_K \tag{8}$$

where P_D and P_K represent the dissipated power due to damping and the power caused by the stiffness variation, respectively. Also, the parameter $\varphi \in \{0, 1\}$ controls the storage of dissipated energy and disables the storage if the energy stored is higher than an upper bound $\bar{T}$, and the parameter $\sigma \in \{\varphi, 1\}$ controls the injection or extraction of energy from the storage. The energy stored is

$$T(z) = \frac{1}{2} z^2 \tag{9}$$

and its time derivative is

$$\dot{T}(z) = z\dot{z} = \varphi P_D - \sigma P_K \tag{10}$$

A lower bound δ is used for the minimum amount of energy stored. In addition, to avoid singularities, $z(t = 0) > 0$ with $T(z(0)) \geq \delta$. Then, the authors in [3], [4] showed that the system is passive with respect to the pair $(F^{\text{ext}}, \dot{\xi})$ if $T(t) \geq \delta$, where $F^{\text{ext}} \in \mathbb{R}^6$ is the external force and $\xi \in SE(3)$ is the end-effector pose of the robot.

III. Method

We aim to formulate a state-feedback controller (2) that allows safe kinesthetic teaching. Here, the nominal state-feedback controller, k^d, represents the robot's desired Cartesian compliant behavior. Then, the robot's compliant behavior is modified by a quadratic optimization problem (7) to ensure that the robot's states stay in a safe set.

A. Robot System

The rigid-body dynamics of the robot can be written in the joint space of the robot, $q \in \mathbb{R}^n$, as [12]

$$M(q)\ddot{q} + C(q,\dot{q})\dot{q} + G(q) = \tau + \tau^{\text{ext}} \tag{11}$$

where $M(q) \in \mathbb{R}^{n \times n}$ is the generalized inertia matrix, $C(q,\dot{q}) \in \mathbb{R}^{n \times n}$ describes the Coriolis and centripetal forces effects, $G(q) \in \mathbb{R}^n$ captures the gravity-induced torques, and $\tau \in \mathbb{R}^n$ represents the input torques, n being the number of joints of the robot. Finally, $\tau^{\text{ext}} \in \mathbb{R}^n$ represents the external torques.

The rigid-body equation of the robot can be written in terms of its end-effector pose, ξ, which is composed by the end-effector's position and orientation:

$$M_\xi(q)\ddot{\xi} + C_\xi(q,\dot{q})\dot{\xi} + G_\xi(q) = F + F^{\text{ext}} \tag{12}$$

where $F \in \mathbb{R}^6$ is the input force, and, for a fully-actuated robot ($n = 6$), $M_\xi \in \mathbb{R}^{6\times6}$, $C_\xi \in \mathbb{R}^{6\times6}$, and $G_\xi \in \mathbb{R}^6$ are equal to

$$M_\xi = J^{-\mathrm{T}}(q) M(q) J^{-1}(q) \tag{13}$$

$$C_\xi = J^{-\mathrm{T}}(q)(C(q,\dot{q}) - M(q)J^{-1}(q)\dot{J}(q))J^{-1}(q) \tag{14}$$

$$G_\xi = J^{-\mathrm{T}}(q) G(q) \tag{15}$$

assuming that the Jacobian relative to the base frame of the robot, $J(q) \in \mathbb{R}^{6\times6}$, has full rank [13].

By applying partial feedback linearization [14, Ch. 9], we can write the input, $u \in \mathbb{R}^6$, to the system as the gravity-compensated force:

$$u = F + F^{\text{ext}} - G_\xi(q) \tag{16}$$

Then, by choosing the state vector as $x = [\xi^{\mathrm{T}}, \dot{\xi}^{\mathrm{T}}]^{\mathrm{T}} \in \mathbb{R}^{12}$, the linearized system is

$$\dot{x} = A(q,\dot{q})x + B(q)u \tag{17}$$

where

$$A = \begin{bmatrix} 0_6 & I_6 \\ 0_6 & -M_\xi^{-1}(q) C_\xi(q,\dot{q}) \end{bmatrix}, \; B = \begin{bmatrix} 0_6 \\ M_\xi^{-1}(q) \end{bmatrix} \tag{18}$$

Lemma III.1. *$M_\xi(q)$ is invertible since $J(q)$ is also invertible.*

Proof: We know that $M(q)$ is invertible because $M(q)$ is a symmetric positive-definite matrix ($M(q) \in S^n_{++}$) [12]. Then, it can be obtained from (13) that

$$M_\xi^{-1}(q) = (J^{-\mathrm{T}}(q) M(q) J^{-1}(q))^{-1} = J(q) M^{-1}(q) J^{\mathrm{T}}(q) \tag{19}$$

which holds since we have assumed that $J(q)$ has full rank to formulate the rigid-body equation (12). ∎

B. Cost Function

The nominal state-feedback controller (2), $k^d \in \mathbb{R}^6$, should achieve the robot's desired Cartesian compliant behavior. A Cartesian impedance controller [15] is used to establish a mass-spring-damper relationship between the Cartesian pose variation from its reference, $\Delta\xi = \xi_d - \xi$, ξ_d being the Cartesian reference, and the external Cartesian force, F^{ext}:

$$F^{\text{ext}} = M_\xi(q)\ddot{\xi} + (D + C_\xi(q,\dot{q}))\dot{\xi} - K\Delta\xi \tag{20}$$

where D and K are the virtual damping and stiffness matrices, respectively. The virtual inertia is chosen equal to the

robot inertia, $M_\xi(q)$, to avoid inertia shaping [16, Ch. 3.2], so that the input force F does not require feedback from the external forces and is equal to

$$F = K\Delta\xi - D\dot{\xi} + G_\xi(q) \tag{21}$$

Therefore, the gravity-compensated nominal state-feedback controller is

$$k^d = K\Delta\xi - D\dot{\xi} + F^{\text{ext}} \tag{22}$$

and we can formulate a new cost function analogous to the cost function in (7),

$$L(\xi, \dot{\xi}, u, F^{\text{ext}}) = \frac{1}{2}\left|\left|u - K\Delta\xi + D\dot{\xi} - F^{\text{ext}}\right|\right|_2^2 \tag{23}$$

Then, the cost function (23) can be expressed in terms of the states and inputs of the system, assuming that $\dot{\xi}_d = 0$, $(x - x_d) = \left[-\Delta\xi^{\text{T}}, \dot{\xi}^{\text{T}}\right]^{\text{T}}$:

$$L(x, u, F^{\text{ext}}) = \frac{1}{2}\left|\left|u + \left[K, D\right](x - x_d) - F^{\text{ext}}\right|\right|_2^2 \tag{24}$$

C. Inequality Constraint

A safety function can be formulated to ensure that the safety distance is always greater or equal than the current distance to the obstacles subtracted by the distance needed to brake the system into a full stop with constant and instantaneous acceleration [6], [8]. For our problem, each of these three elements can be formulated as:

- The safety distance D_s is a constant parameter that can be formulated as

$$D_s = r_{rb} + r_o \tag{25}$$

  where r_{rb} and r_o are the radii of two protective spheres around the robot end-effector and an obstacle that represents the undesired part of the workspace, respectively.
- The current distance $||\Delta\rho||$ is defined using the difference between the robot end-effector position and the obstacle's position,

$$\Delta\rho = \rho - \rho_o \tag{26}$$

  where $\rho = \left[\xi_x, \xi_y, \xi_z\right]^{\text{T}}$ is the robot's position vector and $\rho_o = \left[\xi_{o,x}, \xi_{o,y}, \xi_{o,z}\right]^{\text{T}}$ is the position of the obstacle. The parameters in ρ_o are constant parameters, since we are considering a static (or semi-static) obstacle.
- The distance needed to brake the robot to full stop is slightly more elaborated. For a constant acceleration, $a_{\text{br}} > 0$, the total distance between a final position ρ_{F} and an initial position ρ_0 after an elapsed time t of an object that starts at ρ_0 with relative velocity $v_{\text{rel}} < 0$ is

$$||\rho_{\text{F}} - \rho_0|| = -v_{\text{rel}}t - \frac{1}{2}a_{\text{br}}t^2 \tag{27}$$

  and since the time to brake to full stop is $t = -v_{\text{rel}}/a_{\text{br}}$, the braking distance is equal to

$$||\rho_{\text{F}} - \rho_0|| = \frac{v_{\text{rel}}^2}{2a_{\text{br}}} \tag{28}$$

  v_{rel} being the velocity prior to braking in the direction of the obstacle,

$$v_{\text{rel}} = \frac{\Delta\rho^{\text{T}}}{||\Delta\rho||}v \tag{29}$$

  where $v = \left[\dot{\xi}_x, \dot{\xi}_y, \dot{\xi}_z\right]^{\text{T}}$. Also, a_{br} is a parameter defined by the user that other authors commonly define as the maximum braking ability of the robot [6], [8]. However, one could decide to choose a smaller value to have even larger margins.

Finally, the safety function is formulated as

$$D_s \geq ||\Delta\rho|| - \frac{v_{\text{rel}}^2}{2a_{\text{br}}} \tag{30}$$

so the SCBF candidate $h : \mathbb{R}^n \to \mathbb{R}$ is

$$h(x) = \sqrt{2a_{\text{br}}(||\Delta\rho|| - D_s)} + \frac{\Delta\rho^{\text{T}}}{||\Delta\rho||}v \tag{31}$$

In addition, we know that

$$\frac{d(||\Delta\rho||)}{dt} = v_{\text{rel}} = \frac{\Delta\rho^{\text{T}}}{||\Delta\rho||}v \tag{32}$$

and from the system's model (17), (18),

$$\frac{d(\Delta\rho)}{dt} = v \tag{33}$$

$$\frac{dv}{dt} = -\Phi v + \Gamma\left[I_3, 0_3\right]u \tag{34}$$

where

$$\Phi = \left(M_\xi^{-1}(q)C_\xi(q, \dot{q})\right)_{[1:3,1:3]} \in \mathbb{R}^{3\times3} \tag{35}$$

$$\Gamma = \left(M_\xi^{-1}(q)\right)_{[1:3,1:3]} \in \mathbb{R}^{3\times3} \tag{36}$$

are submatrices composed by the first three rows and columns of their original matrices (Matlab notation). Then, considering that

$$\frac{d\left(\sqrt{2a_{\text{br}}(||\Delta\rho|| - D_s)}\right)}{dt} = \frac{a_{\text{br}}}{\sqrt{2a_{\text{br}}(||\Delta\rho|| - D_s)}}\frac{d(||\Delta\rho||)}{dt} \tag{37}$$

and

$$\frac{d\left(\frac{\Delta\rho^{\text{T}}}{||\Delta\rho||}v\right)}{dt} = \frac{d\left(\frac{\Delta\rho^{\text{T}}}{||\Delta\rho||}\right)}{dt}v + \frac{\Delta\rho^{\text{T}}}{||\Delta\rho||}\frac{dv}{dt} \tag{38}$$

with

$$\frac{d\left(\frac{\Delta\rho^{\text{T}}}{||\Delta\rho||}\right)}{dt}v = \left(\frac{v^{\text{T}}}{||\Delta\rho||} - \frac{\Delta\rho^{\text{T}}v\Delta\rho^{\text{T}}}{||\Delta\rho||^3}\right)v \tag{39}$$

the time derivative of $h(x)$ in (31) is equal to

$$\frac{dh(x)}{dt} = \frac{a_{\text{br}}\Delta\rho^{\text{T}}v}{||\Delta\rho||\sqrt{2a_{\text{br}}(||\Delta\rho|| - D_s)}} + \frac{\Delta\rho^{\text{T}}\Gamma\left[I_3, 0_3\right]u}{||\Delta\rho||} - \frac{\Delta\rho^{\text{T}}\Phi v}{||\Delta\rho||} + \frac{||v||^2}{||\Delta\rho||} - \frac{(\Delta\rho^{\text{T}}v)^2}{||\Delta\rho||^3} \tag{40}$$

Therefore, to fulfill the condition (6) that ensures that the safe set is forward invariant, we must satisfy the inequality constraint

$$\frac{a_{\mathrm{br}}\Delta\rho^{\mathrm{T}}v}{||\Delta\rho||\sqrt{2a_{\mathrm{br}}(||\Delta\rho||-D_s)}}+\frac{\Delta\rho^{\mathrm{T}}\Gamma\left[I_3,\,0_3\right]u}{||\Delta\rho||} -\frac{\Delta\rho^{\mathrm{T}}\Phi v}{||\Delta\rho||}+\frac{||v||^2}{||\Delta\rho||}-\frac{(\Delta\rho^{\mathrm{T}}v)^2}{||\Delta\rho||^3}+\gamma h^Z\geq 0 \tag{41}$$

which can be rewritten as

$$A_{\mathrm{CBF}}u\leq b_{\mathrm{CBF}} \tag{42}$$

where

$$A_{\mathrm{CBF}}=-\Delta\rho^{\mathrm{T}}\Gamma\left[I_3,\,0_3\right] \tag{43}$$

$$b_{\mathrm{CBF}}=\frac{a_{\mathrm{br}}\Delta\rho^{\mathrm{T}}v}{\sqrt{2a_{\mathrm{br}}(||\Delta\rho||-D_s)}}+||v||^2-\frac{(\Delta\rho^{\mathrm{T}}v)^2}{||\Delta\rho||^2} +||\Delta\rho||\gamma h^Z-\Delta\rho^{\mathrm{T}}\Phi v \tag{44}$$

D. Discrete-Time QP Problem Implementation

The discrete-time implementation of the nominal state-feedback controller in (22) allows to obtain the input at time-step i by using the robot state (x_i) and the estimated external force ($\hat{F}_i^{\mathrm{ext}}$) at the same time-step. Therefore, the only free variable of the cost function in (24) is u_i,

$$L(u_i)=\frac{1}{2}\left|\left|u_i+\left[K,\,D\right](x_i-x_{d,i})-\hat{F}_i^{\mathrm{ext}}\right|\right|_2^2 \tag{45}$$

The cost function in (45) can be reduced (by eliminating its constant terms) to a standard Quadratic Program (QP) problem:

$$L_r(u_i)=\frac{1}{2}u_i^{\mathrm{T}}Qu_i+c^{\mathrm{T}}u_i \tag{46}$$

where $Q=I_6$ and $c^{\mathrm{T}}=\left[K,\,D\right](x_i-x_{d,i})-\hat{F}_i^{\mathrm{ext}}$. It is trivial to see that the quadratic term of the cost function in (46) is positive definite, $Q\in S_{++}^n$.

Moreover, similar to the cost function (46), A_{CBF} and b_{CBF} of the SCBF-based inequality constraint (42) only depend on x_i and therefore they can be treated as constants at each time-step for this problem. Therefore, analogous to (7), the QP problem to online modify the robot's compliant behavior at each time-step i is

$$\begin{aligned} k_i=&\arg\,\min\nolimits_{u_i\in\mathbb{R}^6}L_r(u_i)\\ &\text{s.t.}\;\; A_{\mathrm{CBF}}u_i\leq b_{\mathrm{CBF}}\end{aligned} \tag{47}$$

E. Varying the Compliant Behavior of the System

If the inequality constraint (42) of the QP problem is active, the cost function (46) will not be equal to zero ($L_r(u)>0$). In this case, since $u\neq k^d-G_\xi(q)$, the relationship between the Cartesian pose variation from its reference and the external Cartesian force (20) is modified,

$$F^{\mathrm{ext}}=M_\xi(q)\ddot{\xi}+(D+C_\xi(q,\dot{q}))\dot{\xi}-K\Delta\xi-\Delta u \tag{48}$$

Then, the additional force Δu can used to vary the stiffness and damping parameters,

$$K'(t)=K+\Delta K(t) \tag{49}$$

$$D'(t)=D+\Delta D(t) \tag{50}$$

where $K',D'\in S_{++}^n$, and

$$\Delta u=\Delta K\Delta\xi-\Delta D\dot{\xi} \tag{51}$$

To vary the Cartesian compliance parameters in a stable manner, we first show that, using an approach based on [17], the nominal state-feedback controller (22) is stable.

Lemma III.2. *The time-varying Lyapunov function*

$$V(x,t)=\frac{1}{2}\dot{\xi}^{\mathrm{T}}M_\xi(q)\dot{\xi}+\frac{1}{2}\Delta\xi^{\mathrm{T}}K\Delta\xi-\alpha\Delta\xi^{\mathrm{T}}M_\xi(q)\dot{\xi} \tag{52}$$

where $x=\left[\Delta\xi^{\mathrm{T}},\,\dot{\xi}^{\mathrm{T}}\right]^{\mathrm{T}}$*, shows the global asymptotic stability of the nominal state-feedback controller* k^d *in (22) for* $\alpha>0$ *satisfying*

$$\min\left(\sqrt{\frac{\lambda_{m,K}}{\lambda_{M,M_\xi}}},\;\frac{2\lambda_{m,K}}{\lambda_{M,D}},\;\frac{\lambda_{m,D}}{2(\lambda_{M,M_\xi}+k_C||\Delta\xi||)}\right)>\alpha \tag{53}$$

where $\lambda_{m,\Pi}$ *and* $\lambda_{M,\Pi}$ *are the smallest and largest eigenvalues of a matrix* Π*, respectively, and* k_C *is a positive constant such that for all* $x,y,z\in\mathbb{R}^n$ *[17]*

$$||C_\xi(x,y)z||\leq k_C||y||||z|| \tag{54}$$

Proof: See Appendix. ∎

Then, since $M_\xi(q)$, K, $D\in S_{++}^n$, a passive map from the external force F^{ext} to the velocity $\dot{\xi}$ is guaranteed,

$$\dot{V}<\dot{\xi}^{\mathrm{T}}F^{\mathrm{ext}}-\frac{1}{2}\left[\dot{\xi}-\alpha\Delta\xi\right]^{\mathrm{T}}D\left[\dot{\xi}-\alpha\Delta\xi\right]<\dot{\xi}^{\mathrm{T}}F^{\mathrm{ext}} \tag{55}$$

where the passivity condition valid for passive environments is

$$V(t)-V(0)<\int_0^t\dot{\xi}^{\mathrm{T}}(\tau)F^{\mathrm{ext}}(\tau)d\tau \tag{56}$$

However, the additional force Δu (51) produces extra energy, which can break the passivity of the system if the additional energy that is injected into the system causes a positive variation of the stiffness, $\dot{K}'(t)>0$. Defining H as a Lyapunov function that is equivalent to considering (52) with time-varying $K'(t)$ and $D'(t)$, its time derivative is

$$\dot{H}<\dot{\xi}^{\mathrm{T}}F^{\mathrm{ext}}-P_D+P_K \tag{57}$$

where

$$P_D=\frac{1}{2}\left[\dot{\xi}-\alpha\Delta\xi\right]^{\mathrm{T}}D'\left[\dot{\xi}-\alpha\Delta\xi\right] \tag{58}$$

$$P_K=\frac{1}{2}\Delta\xi^{\mathrm{T}}\dot{K}'\Delta\xi \tag{59}$$

Then, a storage function for the system can be defined as

$$W=H+T \tag{60}$$

where T is the energy stored in a reservoir (9), as in [3], [4]. The time derivative of W is equal to

$$\dot{W}=\dot{H}+\dot{T}<\dot{\xi}^{\mathrm{T}}F^{\mathrm{ext}}-(1-\varphi)P_D+(1-\sigma)P_K \tag{61}$$

Choosing, as in [4], that $\sigma=1$ when $\dot{K}'(t)>0$,

$$\dot{W}<\dot{\xi}^{\mathrm{T}}F^{\mathrm{ext}} \tag{62}$$

Therefore, analogous to (56), the passivity condition valid for passive environments is

$$W(t) - W(0) < \int_0^t \dot{\xi}^{\mathrm{T}}(\tau) F^{\mathrm{ext}}(\tau) d\tau \tag{63}$$

Moreover, enough stored energy in the reservoir is needed to ensure passivity. We can use the following metric for an arbitrary time interval $[t_s, t_f]$ to ensure that the storage does not get empty [3], [4],

$$T(t_f) = T(t_s) + \int_{t_s}^{t_f} P_D d\tau - \int_{t_s}^{t_f} P_K d\tau \geq \delta \tag{64}$$

which gives

$$T(t_s) - \delta \geq - \int_{t_s}^{t_f} P_D d\tau + \int_{t_s}^{t_f} P_K d\tau \tag{65}$$

The energy needed to increase the stiffness is equal to

$$\int_{t_s}^{t_f} P_K d\tau = \frac{1}{2} \Delta\xi^{\mathrm{T}} \Delta K \Delta\xi \tag{66}$$

whereas the energy that we can inject into the reservoir in the time interval $[t_s, t_f]$ is

$$\int_{t_s}^{t_f} P_D d\tau = \frac{\eta}{2} \left[\dot{\xi} - \alpha\Delta\xi\right]^{\mathrm{T}} D' \left[\dot{\xi} - \alpha\Delta\xi\right] \tag{67}$$

with $\eta = t_f - t_s$ being the duration of the time interval $[t_s, t_f]$. Therefore, as long as $K'(t), D'(t) \in S^n_{++}$ and (51) is satisfied, the virtual damping coefficient, $D' = D + \Delta D(t)$, can be increased with $\Delta D(t) \geq 0$ to ensure that the energy storage does not get empty, (65), if the stiffness variation is too high.

IV. Experiments

In this section, we present the experiments performed to evaluate the proposed method for a kinesthetic teaching application.

A. Application Scenario

The application scenario that motivated the experiments regards automatic quality-assurance processes in the food-packaging industry using images recorded from a camera mounted onto the end-effector of a robot [18], [19]. Since the distance needed between the camera mounted on the robot and the food item for a correct food-quality analysis is unknown, and varies for different types of food, the trajectory of the robot has to be varied. Then, for each type of food, a human operator can be used to manually guide the robot arbitrarily close to the food item for robot trajectory reprogramming, while ensuring that a collision between the end-effector and the food item does not occur, so that neither of the two is damaged.

B. Experimental Setup

The performed experiments consisted of a robot motion in which, during the robot's trajectory execution, a human operator manually guided the robot to bring it arbitrarily close to the object of interest, here, an egg. The experiment was performed using the Panda robot by Franka Emika [20] mounted on a table (see Fig. 1). This robot had seven rotational joints, but since the formulation for the proposed method was focused on fully-actuated non-redundant robots, we locked the last joint ($\theta_7 = -\pi/2$ rad), and then the robot used six degrees of freedom, $n = 6$.

Fig. 1. Setup for the kinesthetic teaching task described in Sec. IV-B. A Franka Emika Panda robot is mounted on a table. The blue piece allows to attach a camera to the robot's end effector. The human operator is manually guiding the robot and displacing it away from its original trajectory and arbitrarily close to the object of interest, here, an egg.

Moreover, the initial impedance parameters used were:

- The initial virtual stiffness K was equal to 250 $[\mathrm{N/m}]$ for the translational degrees of freedom and equaled to 10 $[\mathrm{N/rad}]$ for the rotational degrees of freedom.
- The initial virtual damping D was equal to $2\sqrt{K}$ for all degrees of freedom.

Furthermore, the choice of additional parameters used for the inequality constraint of the quadratic optimization problem (47) were: $\gamma = 1$, $Z = 3$, $D_s = 0.05$ m, and $a_{\mathrm{br}} = 10\ \mathrm{m/s^2}$ (a_{br} was chosen conservatively, since its maximum value was configuration-dependent). Note that γ must be a positive number and Z must be a positive odd integer to guarantee safety [6]. Also, a new quadratic optimization problem was solved every 1 ms, since the sampling rate of the robot was 1 kHz.

V. Results

In this section, we evaluate the results obtained from the experiments described in Sec. IV. First, Fig. 2 shows a 3D representation of the path $\rho(t)$ traversed by the robot. It can be seen how the external force generated by the human operator displaced the robot from its unperturbed path $\rho_{\mathrm{un}}(t)$, where no external force acted on the robot. The robot was able to avoid the undesired parts of its workspace even when the operator was manually guiding the robot, which was

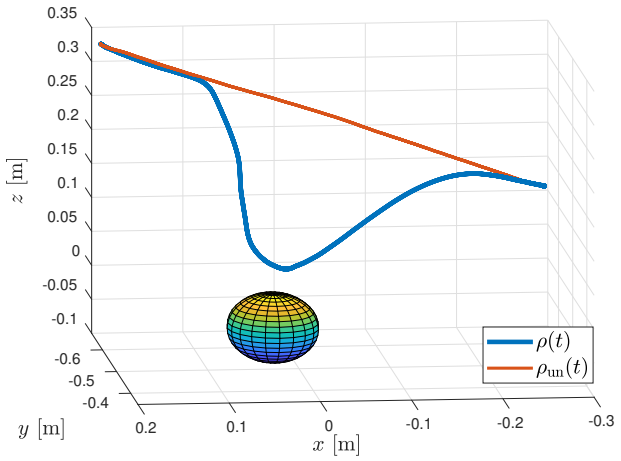

Fig. 2. 3D plot of the path $\rho(t)$ traversed by the robot's end-effector. The operator displaced the robot from its unperturbed path $\rho_{\text{un}}(t)$. The plotted sphere is centered at the obstacle (egg) at ρ_o, and its radius is equal to D_s.

ensured by solving the quadratic optimization problem in (47) at each time-step.

Moreover, Fig. 3 shows the temporal evolution of the safety control barrier function h. It can be seen how the robot end-effector stayed inside the forward-invariant safe set (3), $h(x) \geq 0$, throughout the entire trajectory, thus confirming that undesired parts of the robot's workspace were avoided using the proposed method.

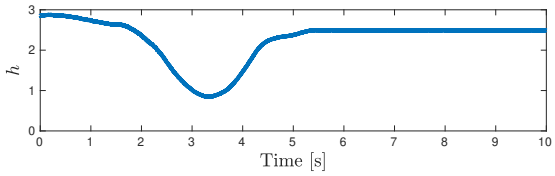

Fig. 3. Temporal variation of the SCBF, $h(x)$ in (31), throughout the experiment.

Furthermore, as mentioned in Sec. III-E, the solution of the quadratic optimization problem (47) was used to online modify the impedance parameters of the Cartesian compliance controller to avoid undesired parts of the robot's workspace. Figure 4 shows the temporal variation of the external force, as well as the stable temporal variation of the virtual stiffness during the trajectory segment where the inequality constraint of the QP optimization problem (47) was active ($t = 2.658$ s to $t = 3.575$ s). Then, Fig. 5 shows the temporal variation of the joint input torques τ, which were commanded to the robot to achieve the virtual stiffness variation seen in Fig. 4. Figure 5 also shows the unmodified input torques τ_{un} that would be commanded for a constant virtual stiffness, $K' = K$ in (49). It can be seen, in both Figs. 4 and 5, how the nominal controller of the robot was only modified when needed in a minimally-invasive fashion. Therefore, when the SCBF-based inequality constraint (47) was not active, *i.e.*, before $t = 2.658$ s and after $t = 3.575$ s, the desired compliant behavior of the robot, $K' = K$ and $D' = D$, was achieved. Additionally, in this experiment, the virtual stiffness K' in (49) was modified while leaving the virtual damping constant $D' = D$ in (50).

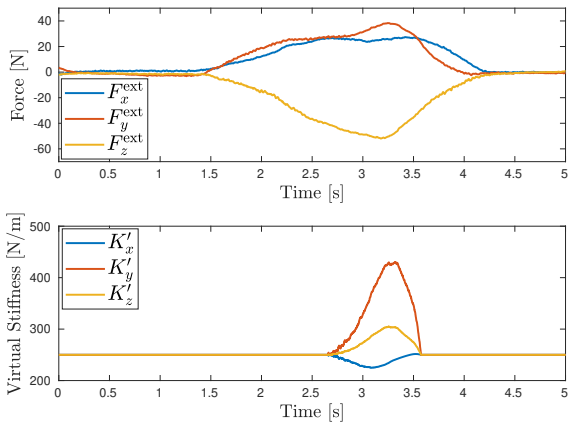

Fig. 4. Temporal variation of the external force and the virtual stiffness throughout the experiment.

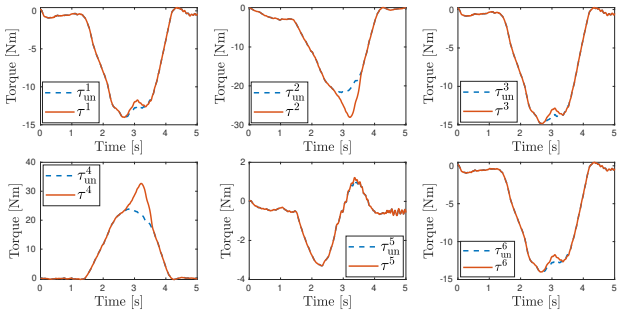

Fig. 5. Temporal variation of the input torques τ^j, compared to the unmodified (*i.e.*, without SCBF-based compliance variation) input torques τ_{un}^j for each joint $j \in \{1, \ldots, 6\}$, throughout the experiment.

VI. Discussion

In this paper, we have proposed a method to modify the Cartesian compliance parameters of a robot to avoid that human operators manually guide a robot to undesired parts of its workspace in the context of safe kinesthetic teaching. The proposed method modifies a nominal controller, whose goal is to achieve the desired compliant behavior of the robot, using an SCBF as an inequality constraint of a QP problem to ensure forward invariance of the safe set of robot states.

Prior to the formulation of SCBF-based methods, artificial potential fields have been used for robot obstacle avoidance [11]. However, SCBFs have recently gained popularity, since they ensure formal guarantees for obstacle avoidance. Also, while potential fields do not emphasize optimality [21], SCBFs are minimally invasive and only modify the nominal controller behavior if needed [5], as illustrated in Sec. V. In addition, the main appeal of artificial potential fields is the low computational loads needed, but fast problem-solving is also guaranteed for our method, since the proposed

QP problem (47) is a convex problem with positive definite quadratic term, $Q \in S^n_{++}$: using a convex optimization solver such as CVXGEN [22] with C++ to solve (47) took on average 5.2 μs with an standard deviation of 3.1 μs using a single PC (Intel Xeon CPU E3-1245, 3.7 GHz, 4 cores, 64-bit).

Moreover, several authors have formulated SCBFs as inequality constraints of a QP problem for obstacle avoidance in robot manipulators [7]–[10]. However, it is a novelty of our proposed method to explicitly take the rigid-body dynamics of the robot into consideration: [7] and [8] considered the robot kinematics, [9] included a simplified version of the dynamics that neglects the Coriolis and centripetal forces, and [10] performed a purely kinematic implementation of a SCBF but guarantees safety at the level of dynamics by incorporating kinetic energy to the SCBF. The benefit of considering the robot dynamics when formulating our SCBF is that adherence to the constraints can be guaranteed [9], as illustrated by the experiments performed (see Fig. 3). In contrast, SCBF-based constraint violations may occur for a kinematic formulation depending on the choice of the optimization parameters, as illustrated in [10]. Also, slight constraint violations were observed in [9] for a simplified-dynamics formulation.

Furthermore, an additional benefit of using an explicit formulation of the dynamic model of the robot is that it allows to quantify the additional Cartesian force, Δu in (48), required to modify the nominal state-feedback controller k^d to ensure safety. It is a novelty of the proposed method to calculate the required variation of the Cartesian compliant behavior of the system (as shown in Fig. 4) that is necessary to achieve this additional force (49)–(51), so that SCBF-based constraints are satisfied. This is relevant for kinesthetic teaching applications, *e.g.*, in the scenario shown in Sec. IV, since it indicates the changes in the robot's compliant behavior toward external force that human operators would feel when manually guiding the robot. Another example of a kinesthetic teaching scenario where our method may be relevant is for avoiding potential collisions occurring when an operator guides a robot with a sensitive object grasped in its end-effector.

Finally, previous works [7]–[10] where a robot nominal controller was modified using SCBFs focused on the stability guarantees of the nominal controller. In addition, we provided global asymptotic stability guarantees of convergence to the robot's desired state for the modified controller obtained from the QP problem. We used a passivity-based energy-storage formulation to ensure that the variation of the Cartesian compliance parameters determined by the proposed method is stable. This formulation has previously been used for a robot puncturing task through a three-layers box that simulated the varying stiffness of a human body [3], and also to allow stable robot controller-switching between position control and compliance control [4]. Therefore, its use in showing stability for SCBF-based modifications of a nominal controller is novel. In addition, our contribution to this energy-storage formulation, as presented in Lemma III.2 (Sec. III-E) and its proof (Appendix), is to replace the nonstrict Lyapunov function used in [3], [4] by a Lyapunov function with strictly negative time-derivative to ensure the strict stability of our method. As a trade-off, the power available to fill the energy storage, P_D in (58), is smaller for our method.

VII. Conclusion

Safety control barrier functions have been used to online modify the Cartesian compliant behavior of a robot in a strictly stable manner (global asymptotic stability), so as to avoid that human operators manually guide a robot's end-effector to undesired parts of its workspace in the context of safe kinesthetic teaching. The rigid-body dynamics of the robot is considered in our method to guarantee adherence to the safety constraints. The proposed method has been successfully evaluated through experiments using a Franka Emika Panda robot for a kinesthetic teaching application.

References

[1] C. Schou, J. Damgaard, S. Bøgh, and O. Madsen, "Human-robot interface for instructing industrial tasks using kinesthetic teaching," in *44th IEEE International Symposium on Robotics (ISR)*. Seoul, Korea: IEEE, Oct. 19–27, 2013, pp. 1–6.

[2] M. Karlsson, A. Robertsson, and R. Johansson, "Autonomous interpretation of demonstrations for modification of dynamical movement primitives," in *IEEE International Conference on Robotics and Automation (ICRA)*, Singapore, 29 May–2 Jun. 2017, pp. 316–321.

[3] F. Ferraguti, C. Secchi, and C. Fantuzzi, "A tank-based approach to impedance control with variable stiffness," in *IEEE International Conference on Robotics and Automation (ICRA)*, Karlsruhe, Germany, May 6–10, 2013, pp. 4948–4953.

[4] C. T. Landi, F. Ferraguti, C. Fantuzzi, and C. Secchi, "A passivity-based strategy for coaching in human-robot interaction," in *IEEE International Conference on Robotics and Automation (ICRA)*. Brisbane, Australia: IEEE, May 21–25, 2018, pp. 3279–3284.

[5] A. D. Ames, S. Coogan, M. Egerstedt, G. Notomista, K. Sreenath, and P. Tabuada, "Control barrier functions: Theory and applications," in *European Control Conference (ECC)*. Naples, Italy: IEEE, Jun. 25–28, 2019, pp. 3420–3431.

[6] L. Wang, A. D. Ames, and M. Egerstedt, "Safety barrier certificates for collisions-free multirobot systems," *IEEE Transactions on Robotics*, vol. 33, no. 3, pp. 661–674, 2017.

[7] C. T. Landi, F. Ferraguti, S. Costi, M. Bonfè, and C. Secchi, "Safety barrier functions for human-robot interaction with industrial manipulators," in *European Control Conference (ECC)*. Naples, Italy: IEEE, Jun. 25–28, 2019, pp. 2565–2570.

[8] F. Ferraguti, M. Bertuletti, C. T. Landi, M. Bonfè, C. Fantuzzi, and C. Secchi, "A control barrier function approach for maximizing performance while fulfilling to ISO/TS 15066 regulations," *IEEE Robotics and Automation Letters*, vol. 5, no. 4, pp. 5921–5928, 2020.

[9] M. Rauscher, M. Kimmel, and S. Hirche, "Constrained robot control using control barrier functions," in *IEEE/RSJ International Conference on Intelligent Robots and Systems (IROS)*. Daejeon, Korea: IEEE, Oct. 9–14, 2016, pp. 279–285.

[10] A. Singletary, S. Kolathaya, and A. D. Ames, "Safety-critical kinematic control of robotic systems," *IEEE Control Systems Letters*, 2021.

[11] O. Khatib, "Real-time obstacle avoidance for manipulators and mobile robots," in *IEEE International Conference on Robotics and Automation (ICRA)*, vol. 2, St. Louis, USA, Mar. 25–28, 1985, pp. 500–505.

[12] B. Siciliano and O. Khatib, *Springer Handbook of Robotics*, 2nd ed. Springer, Berlin, Germany, 2016.

[13] O. Khatib, "A unified approach for motion and force control of robot manipulators: The operational space formulation," *IEEE Journal on Robotics and Automation*, vol. 3, no. 1, pp. 43–53, 1987.

[14] H. K. Khalil, *Nonlinear control*. Pearson Higher Ed., New York, 2014.

[15] N. Hogan, "Impedance control: An approach to manipulation: Parts I–III," *J. Dynamic Syst., Measurement, and Control*, vol. 107, no. 1, pp. 1–24, 1985.

[16] C. Ott, *Cartesian impedance control of redundant and flexible-joint robots*. Springer, Berlin, Germany, 2008.
[17] V. Santibáñez and R. Kelly, "Strict Lyapunov functions for control of robot manipulators," *Automatica*, vol. 33, no. 4, pp. 675–682, 1997.
[18] V. Kakani, V. H. Nguyen, B. P. Kumar, H. Kim, and V. R. Pasupuleti, "A critical review on computer vision and artificial intelligence in food industry," *Journal of Agriculture and Food Research*, vol. 2, p. 100033, 2020.
[19] L. Zhu, P. Spachos, E. Pensini, and K. N. Plataniotis, "Deep learning and machine vision for food processing: A survey," *Current Research in Food Science*, vol. 4, pp. 233–249, 2021.
[20] *Panda – Data Sheet*, Franka Emika, 2019.
[21] C. Liu and M. Tomizuka, "Algorithmic safety measures for intelligent industrial co-robots," in *IEEE International Conference on Robotics and Automation (ICRA)*. Stockholm, Sweden: IEEE, May 16–21, 2016, pp. 3095–3102.
[22] J. Mattingley and S. Boyd, "CVXGEN: A code generator for embedded convex optimization," *Optimization and Engineering*, vol. 12, no. 1, pp. 1–27, 2012.

APPENDIX
PROOF OF LEMMA III.2

It is noted in [17] that the time-varying Lyapunov function

$$V_1(\xi, \Delta\xi, t) = \frac{1}{2}\dot{\xi}^{\mathrm{T}} M_\xi(q)\dot{\xi} + \frac{1}{2}\Delta\xi^{\mathrm{T}} K \Delta\xi \tag{68}$$

that is often used to show the stability of a Cartesian impedance controller [16, Ch. 3], such as the nominal state-feedback controller k^d (22), is a nonstrict Lyapunov function, *i.e.*, its time derivative is a globally negative-semidefinite function. Then, the authors in [17] have proposed the following alternative Lyapunov candidate to obtain a globally negative-definite time derivative [17]:

$$V_2(x,t) = \frac{1}{2}\dot{\xi}^{\mathrm{T}} M_\xi(q)\dot{\xi} + \frac{1}{2}\Delta\xi^{\mathrm{T}} K \Delta\xi - \alpha f(\Delta\xi)^{\mathrm{T}} M_\xi(q)\dot{\xi} \tag{69}$$

where

$$f(\Delta\xi) = \frac{1}{1 + ||\Delta\xi||}\Delta\xi \tag{70}$$

and $\alpha > 0$ must satisfy

$$\min\left(\sqrt{\frac{\lambda_{m,K}}{\lambda_{M,M_\xi}}},\ \frac{2\lambda_{m,K}}{\lambda_{M,D}},\ \frac{\lambda_{m,D}}{2(k_C + 2\lambda_{M,M_\xi})}\right) > \alpha \tag{71}$$

However, using a scaling factor $f(\Delta\xi)$ in the cross-term of the Lyapunov candidate function can cause slow convergence to the equilibrium point, $\left[\Delta\xi^{\mathrm{T}}, \dot{\xi}^{\mathrm{T}}\right] = 0 \in \mathbb{R}^{2n}$. Therefore, we present a solution based on the work by [17], but removing the scaling factor $f(\Delta\xi)$:

$$V(x,t) = \frac{1}{2}\dot{\xi}^{\mathrm{T}} M_\xi(q)\dot{\xi} + \frac{1}{2}\Delta\xi^{\mathrm{T}} K \Delta\xi - \alpha\Delta\xi^{\mathrm{T}} M_\xi(q)\dot{\xi} \tag{72}$$

The Lyapunov candidate (72) is equivalent to

$$\begin{aligned} V(x) = &\frac{1}{2}\left[\dot{\xi} - \alpha\Delta\xi\right]^{\mathrm{T}} M_\xi(q)\left[\dot{\xi} - \alpha\Delta\xi\right] \\ &+ \frac{1}{2}\Delta\xi^{\mathrm{T}}\left[K - \alpha^2 M_\xi(q)\right]\Delta\xi \end{aligned} \tag{73}$$

Therefore, the Lyapunov candidate is strictly positive ($V(x \neq 0) > 0$ and $V(x = 0) = 0$) for

$$\alpha < \sqrt{\frac{\lambda_{m,K}}{\lambda_{M,M_\xi}}} \tag{74}$$

which ensures $K - \alpha^2 M_\xi(q) > 0$.

Moreover, the time-derivative of the Lyapunov candidate (72) is equal to

$$\begin{aligned} \dot{V}(x) = &-\alpha\Delta\xi^{\mathrm{T}}\left[\dot{M}_\xi(q) - C_\xi(q,\dot{q})\right]\dot{\xi} + \alpha\dot{\xi}^{\mathrm{T}} M_\xi(q)\dot{\xi} \\ &-\dot{\xi}^{\mathrm{T}} D\dot{\xi} - \alpha\Delta\xi^{\mathrm{T}} K\Delta\xi + \alpha\Delta\xi^{\mathrm{T}} D\dot{\xi} \end{aligned} \tag{75}$$

Considering that the matrix $\dot{M}_\xi(q) - 2C_\xi(q,\dot{q})$ is skew symmetric [16, Ch. 2]:

$$\begin{aligned} \dot{V}(x) = &-\alpha\Delta\xi^{\mathrm{T}} C_\xi(q,\dot{q})\dot{\xi} + \alpha\dot{\xi}^{\mathrm{T}} M_\xi(q)\dot{\xi} \\ &-\dot{\xi}^{\mathrm{T}} D\dot{\xi} - \alpha\Delta\xi^{\mathrm{T}} K\Delta\xi + \alpha\Delta\xi^{\mathrm{T}} D\dot{\xi} \end{aligned} \tag{76}$$

Then, defining the upper bound on certain terms:

$$-\dot{\xi}^{\mathrm{T}} D\dot{\xi} \leq -\frac{1}{2}\dot{\xi}^{\mathrm{T}} D\dot{\xi} - \frac{1}{2}\lambda_{m,D}\left|\left|\dot{\xi}\right|\right|^2 \tag{77}$$

$$\alpha\dot{\xi}^{\mathrm{T}} M_\xi(q)\dot{\xi} \leq \alpha\lambda_{M,M_\xi}\left|\left|\dot{\xi}\right|\right|^2 \tag{78}$$

$$-\alpha\Delta\xi^{\mathrm{T}} C_\xi(q,\dot{q})\dot{\xi} \leq \alpha k_C\left|\left|\Delta\xi\right|\right|\left|\left|\dot{\xi}\right|\right|^2 \tag{79}$$

it follows that

$$\begin{aligned} \dot{V}(x) \leq &-\frac{1}{2}\left[\dot{\xi} - \alpha\Delta\xi\right]^{\mathrm{T}} D\left[\dot{\xi} - \alpha\Delta\xi\right] + \frac{1}{2}\alpha^2\Delta\xi^{\mathrm{T}} D\Delta\xi \\ &-\frac{1}{2}\lambda_{m,D}\left|\left|\dot{\xi}\right|\right|^2 - \alpha\Delta\xi^{\mathrm{T}} K\Delta\xi \\ &+\alpha k_C\left|\left|\Delta\xi\right|\right|\left|\left|\dot{\xi}\right|\right|^2 + \alpha\lambda_{M,M_\xi}\left|\left|\dot{\xi}\right|\right|^2 \end{aligned} \tag{80}$$

which can be rewritten as

$$\begin{aligned} \dot{V}(x) \leq &-\frac{1}{2}\left[\dot{\xi} - \alpha\Delta\xi\right]^{\mathrm{T}} D\left[\dot{\xi} - \alpha\Delta\xi\right] \\ &+\alpha\Delta\xi^{\mathrm{T}}\left[\tfrac{\alpha}{2}D - K\right]\Delta\xi - \frac{1}{2}\lambda_{m,D}\left|\left|\dot{\xi}\right|\right|^2 \\ &+\alpha k_C\left|\left|\Delta\xi\right|\right|\left|\left|\dot{\xi}\right|\right|^2 + \alpha\lambda_{M,M_\xi}\left|\left|\dot{\xi}\right|\right|^2 \end{aligned} \tag{81}$$

It can be ensured that the term

$$\alpha\Delta\xi^{\mathrm{T}}\left[\tfrac{\alpha}{2}D - K\right]\Delta\xi \tag{82}$$

is strictly negative for

$$\alpha < \frac{2\lambda_{m,K}}{\lambda_{M,D}} \tag{83}$$

and that the term

$$-\frac{1}{2}\lambda_{m,D}\left|\left|\dot{\xi}\right|\right|^2 + \alpha k_C\left|\left|\Delta\xi\right|\right|\left|\left|\dot{\xi}\right|\right|^2 + \alpha\lambda_{M,M_\xi}\left|\left|\dot{\xi}\right|\right|^2 \tag{84}$$

is strictly negative for

$$\alpha < \frac{\lambda_{m,D}}{2(\lambda_{M,M_\xi} + k_C||\Delta\xi||)} \tag{85}$$

Therefore, if $\alpha > 0$ satisfies (53)

$$\min\left(\sqrt{\frac{\lambda_{m,K}}{\lambda_{M,M_\xi}}},\ \frac{2\lambda_{m,K}}{\lambda_{M,D}},\ \frac{\lambda_{m,D}}{2(\lambda_{M,M_\xi} + k_C||\Delta\xi||)}\right) > \alpha \tag{86}$$

the Lyapunov candidate function $V(x)$ is strictly positive ($V(x \neq 0) > 0$ and $V(x = 0) = 0$) and its time-derivative is strictly negative ($\dot{V}(x) < 0$). ■